LAWRENCE
LIVERMORE
NATIONAL
LABORATORY

UCRL-JRNL-205167

# Satiated relative permeability of variable-aperture fractures

R. L. Detwiler, H. Rajaram, R. J. Glass

July 12, 2004

Physical Review E

**Satiated relative permeability of variable-aperture fractures**

Russell L. Detwiler
Lawrence Livermore National Laboratory
University of California
7000 East Ave., Livermore, California 94551, USA

Harihar Rajaram
Department of Civil, Environmental and Architectural Engineering
University of Colorado
428 UCB, Boulder, Colorado 80309, USA

Robert J. Glass
Flow Visualization and Processes Laboratory
Sandia National Laboratories
Albuquerque, New Mexico 87185, USA

## ABSTRACT

Experimental studies of capillary-dominated displacements in variable-aperture fractures have demonstrated the occurrence of a satiated state at the end of invasion, where significant entrapment of the displaced phase occurs. The structure of this entrapped phase controls the behavior of flow and transport processes in the flowing phase. Recent studies have shown that the areal saturation of the flowing phase at satiation ($S_f$) is largely controlled by a single parameter $C/\gamma$, where $C$, the Curvature number, weighs the mean in-plane interfacial curvature relative to the mean out-of-plane interfacial curvature, and $\gamma$, the coefficient of variation of the aperture field, represents the strength of interface roughening induced by aperture variations. Here we consider the satiated relative permeability ($k_{rs}$) to the flowing phase, which is defined as the relative permeability at satiation, when the defending phase is fully entrapped. The satiated relative permeability is shown to be a well-defined function of $S_f$ over a wide range of $C/\gamma$, ranging from capillary fingering with significant entrapment ($C/\gamma \to 0$) to smooth invasion with very little entrapment ($C/\gamma > 1$). We propose a relationship, based on effective medium theory, for the satiated relative permeability as a function of $S_f$. The predicted relative permeability values are accurate across the entire range of phase structures representative of capillary-dominated displacements in variable-aperture fractures.

## I. INTRODUCTION

The presence of two or more fluids within a fracture reduces the permeability to each phase [1-4]. This reduction in permeability is often represented by the relative permeability, which is the ratio of the permeability in two-phase flow to that in single-phase flow, and varies between 0 and 1. Experiments and simulations have demonstrated that capillary-dominated displacements (i.e. negligible gravity and viscous forces) in statistically homogeneous variable-aperture fractures can result in a satiated condition in which the invading phase spans the fracture and the defending phase is completely entrapped [5-6]. The satiated state corresponds to the end of invasion, unlike the percolation threshold, which corresponds to first breakthrough and spanning of the domain by the invading phase. The satiated state is established over relatively short time scales [5], and can persist within a variable aperture fracture for a very long duration, unless disturbed by external forces or dissolution of the entrapped phase. The flow and transport properties corresponding to the satiated state are thus important to a variety of applied problems. In this paper, our objective is to develop a model for predicting the relative permeability under satiated conditions.

The satiated relative permeability ($k_{rs}$) is controlled by the geometry of the flowing phase at satiation and the statistical properties of the aperture ($a$) field (described by the mean aperture $\langle a \rangle$, standard deviation $\sigma_a$ and correlation length $\lambda$). The phase geometry itself is controlled by the aperture field statistics and fluid properties such as the interfacial tension between the fluids and their contact angles ($\theta$) at the rock surfaces. Recent experimental studies [5] have demonstrated that in-plane interfacial curvature leads to significant smoothing at interfaces. As a result, phase geometries in two-phase flow through fractures can deviate significantly from the behavior predicted by invasion percolation (IP) algorithms that consider only out-of-plane curvature across the local aperture. A modified invasion percolation algorithm (MIP [5]) that accounts for in-plane curvature in addition to the out-of-plane curvature considered in IP better reproduces experimentally observed phase geometries.

Recent theoretical and computational results based on MIP [7] demonstrate that a simple measure of the flowing phase structure at satiation, the areal saturation ($S_f$), depends strongly on the ratio of two dimensionless parameters: $C=\langle a \rangle/(\lambda\cos\theta)$, which weighs the relative influences of mean in-plane and out-of-plane interfacial curvature on the displacement process, and $\gamma=\sigma_a/\langle a \rangle$, the coefficient of variation of the fracture aperture. Thus, for any capillary dominated invasion process in which values of $\langle a \rangle$, $\sigma_a$, $\lambda$, and $\theta$ yield the same value of $C/\gamma$, the resulting entrapped/flowing phase structures will be similar. Effectively, $C$ measures the strength of smoothing at the invading interface due to in-plane curvature, while $\gamma$ measures the strength of roughening caused by random aperture variations, and it is the competition between these mechanisms that controls phase geometry. For $C/\gamma$ well below 1, out-of-plane, aperture-induced curvature dominates, and the phase structure corresponds to IP within a spatially correlated field. As $C/\gamma$ increases, capillary fingers widen to above the spatial correlation length, due to smoothing generated by in-plane curvature. For $C/\gamma$ well above 1, the interface is dominated by in-plane curvature, and thus behaves as though in a Hele-Shaw cell, with little or no entrapment of the defending phase (see **Fig. 1**). Correspondingly, the areal saturation ($S_f$) at satiation ranges from 1 ($C/\gamma >> 1$) to about 0.37 ($C/\gamma -> 0$). In the intermediate range of $C/\gamma$ (~1-10), Glass et al. [7] also observed a non-unique behavior of $S_f$ at satiation with respect to wetting versus non-wetting fluid invasions. This non-unique behavior is due to asymmetry in competition between the smoothing and roughening mechanisms, which results from the asymmetric distribution of $1/a$.

A useful model for $k_{rs}$ should adequately describe behavior across the wide array of entrapped phase structures corresponding to the full range of $C/\gamma$. Nicholl et al. [6] proposed a model for $k_{rs}$, based on effective medium theory, that identified four controlling parameters: a

tortuosity factor, $\gamma$, the areal saturation of the flowing phase, $S_f$, and two parameters that quantify deviations in the mean and variance of the aperture-field statistics within the flowing phase from those in the entire fracture. They calculated values for each of these parameters for 7 satiated phase structures, demonstrating that the tortuosity played the most significant role in determining $k_{rs}$. However, they did not develop relationships for predicting the model parameters based on fracture and fluid properties. We present a modified version of the model presented by Nicholl et al. [6] that uses concepts from continuum percolation theory to develop a relationship between $k_{rs}$ and $S_f$ and explore this relationship over a broad range of $C/\gamma$. Our model leads to general predictive relationships for $k_{rs}$ in terms of fracture and fluid properties. It is important to emphasize the distinction between this relationship and the more commonly used relative permeability-saturation relationship in two-phase flows. The latter involves relative permeabilities at different saturation values corresponding to a single invasion process. In contrast, the $k_{rs}$-$S_f$ relationship does not correspond to a single invasion process. It represents the variation of (satiated) relative permeability $k_{rs}$ with the areal saturation at satiation ($S_f$), which is in turn controlled by $C/\gamma$, the true "independent variable" in this context. The model predictions agree well with computational estimates of relative permeability obtained using flow simulations in partially saturated fractures.

## II. MODEL FOR $k_{rs}$

Our approach is similar to that of Nicholl et al. [6], who proposed a theoretical expression for relative permeability in a variable aperture fracture by modifying a result for the effective transmissivity of a heterogeneous two-dimensional medium [8] to account for impermeable obstructions to the flowing phase [9]. These theoretical expressions are approximations to the true effective transmissivity, in that they invoke the local cubic law, which assumes that pressure gradients across the aperture are negligible. However, Nicholl et al. [6] found that predictions of relative permeability obtained using the local cubic law were within 10% of experimentally measured relative permeabilities. This is evidently because the relative influence of the entrapped phase on the flow structure is substantially larger than the relative differences between the flow structure predicted by the three-dimensional Stokes equations versus the local cubic law. Though Nicholl et al. [6] measured $k_{rs}$ in a range of different phase structures, their experimental phase structures were not generated by systematic phase invasions. In particular, their phase structures did not cover the entire range of $S_f$ corresponding to the full range of $C/\gamma$, and thus did not present a complete picture of $k_{rs}$.

For a saturated variable-aperture fracture, the effective transmissivity obtained by extension of Landau and Lifshitz's [8] result for a heterogeneous conducting medium is:

$$T_{sat} = \frac{\langle a \rangle^3 g}{12\nu}\left(1 - 1.5\,\gamma^2\right) \qquad (1)$$

where $g$ is the gravitational acceleration and $\nu$ is the kinematic viscosity. Note that (1) is a perturbation approximation and is strictly valid for $\gamma$ smaller than 1. For a partially saturated variable-aperture fracture, the effective transmissivity can be expressed as (modified from [6]):

$$T = k_{rs\|}\,\frac{\langle a_f \rangle^3}{12}\left(1 - 1.5\,\gamma_f^2\right) \qquad (2)$$

In (2), the subscript $f$ refers to the flowing phase, so that $S_f$, $\langle a_f \rangle$ and $\gamma_f$ represent respectively, the areal saturation of the flowing phase, and the mean and coefficient of variation of apertures in the region occupied by the flowing phase. The quantity $k_{rs\|}$ in (2) represents the reduction of

permeability obtained in a parallel-plate fracture (or, equivalently, a homogeneous medium) with impermeable obstructions, whose geometries are identical to those of the entrapped phase. Nicholl et al. [6] further reduced $k_{rs||}$ to the product of $\sigma$ and $S_f$, however, we maintain $k_{rs||}$ because it is directly quantified based on concepts from continuum percolation theory, as discussed below.

We define the relative permeability as the ratio of (2) to (1):

$$k_{rs} = k_{rs||} AB \tag{3}$$

such that the flow through a satiated fracture is represented by $Q = k_{rs} T_{sat} W i$, where $W$ is the width of the fracture and $i$ is the hydraulic gradient. In (3), $A$ and $B$ represent the influence of the relative change in the mean and coefficient of variation of the apertures occupied by the flowing phase from the corresponding values in a fully saturated fracture:

$$A = \langle a_f \rangle^3 \big/ \langle a \rangle^3 \qquad B = \left(1 + 1.5\sigma_f^2\right) \big/ \left(1 + 1.5\sigma^2\right) \tag{4}$$

As shown in the next section, the strongest contribution to $k_{rs}$ is from $k_{rs||}$, which is related to the entrapped phase geometry. The term $A$ is next in order of importance and $B$ has a very minor influence on $k_{rs}$. Note that the volumetric saturation of the flowing fluid ($S$) is related to $S_f$ by the relationship $S_f = S \langle a_f \rangle / \langle a \rangle$. We outline approaches for quantifying each of these terms below.

To quantify $k_{rs||}$, we invoke concepts from continuum percolation theory. The typical continuum percolation problem considers percolation and conduction in a homogeneous medium with randomly positioned identical "holes" as the area fraction of the holes is varied. In two dimensions, there cannot be a continuous hole phase across the domain when the conducting phase is above the percolation threshold. Thus, the entrapped defending fluid phase at the satiated state in variable aperture fractures corresponds to the hole phase in continuum percolation. However, unlike in standard continuum percolation, the geometry of the entrapped phase here is irregular, and there is considerable variation in the size, shape, orientation and aspect ratios of individual entrapped blobs (see **Fig. 1(b)-(e)**). The variation of conductivity with area fraction of the hole-phase has been considered extensively for the case of holes with regular shapes, such as circles/ellipses, squares/rectangles and needles [10-14]; see also the discussions presented by [15,16]. In some studies of continuum percolation [14], mixtures of holes with different shapes and sizes have been considered, with the conclusion that a scaled percolation threshold, defined based on excluded area arguments, is almost invariant over a wide range of continuum percolation systems. Garboczi et al. [14] also proposed a universal conductivity curve for two-dimensional continuum percolation systems. Here, we adapt their universal conductivity curve in a slightly modified form, to propose the following relationship between $k_{rs||}$ and $S_f$:

$$k_{rs||} = \left[1 - \frac{1 - S_f}{1 - S_f^*}\right] \left[1 + \frac{1 - S_f}{1 - S_f^*}\right] \Bigg/ \left[1 + \frac{1 - S_f}{t\left(1 - S_{fI}\right)}\right]^t \tag{5}$$

In (5), there are three parameters: $S_f^*$ is the percolation threshold, $S_{fI}$ is the point where the initial slope for a small area fraction of holes crosses the abscissa when extrapolated and $t$ is the conductivity exponent for two-dimensional percolation and continuum percolation, which has a value close to 1.3 [11,14-17]. Both $S_f^*$ and $S_{fI}$ depend on the aspect ratio of the "holes" in general [13,14]. The expression (5) is an interpolant that is consistent with critical behavior near the

percolation threshold ( $k_{rs||} \sim (S_f - S_f^*)^t$ as $S_f$ approaches $S_f^*$ ) and linear behavior for $S_f$ near 1 ( $k_{rs||} \sim 1 - (1-S_f)/(1-S_{fl})$ ), two limits that are universally observed for continuum percolation [13,14].

The secondary term in (3), $A$, represents the influence of the relative change in mean aperture within the flowing phase. Thus we expect $A > 1$ for non-wetting fluid flow and $A < 1$ for wetting fluid flow. $A$ is also expected to depend strongly on $\sigma$, particularly for small values of $C$. For $C$=0 (IP in a correlated lattice), the fluid phase geometries do not vary with $\sigma$. However, because of selective occupancy of the aperture distribution, the mean aperture within the flowing phase, and thus $A$, will be influenced by $\sigma$. For standard percolation (SP), the invading phase occupies apertures strictly in ascending (wetting) or descending (non-wetting) order, which allows development of an analytical expression for $A$. However, this analytical expression does not provide satisfactory estimates of $A$ for phase structures generated by MIP in two-dimensional variable-aperture fractures, where in-plane curvature effects lead to significant deviations from the assumption of sequential occupancy. Therefore, we propose an empirical relationship for $A$ based on an analysis of aperture field statistics within the invading phase, over a large number of invasion simulations described in detail in the following section:

$$A = 1 \pm b\sigma\left(1 - S_f\right)^2 \qquad (6)$$

where $b$ is a fitted parameter. The last term $B$ in (3), which is a measure of the change in aperture variance from the saturated state to the satiated state has a very minor influence, and thus we have not developed an analytical or empirical relationship to quantify the influence of $B$ on $k_{rs}$.

## III. EVALUATION OF THE $k_{rs}$-$S_f$ MODEL

To evaluate the effectiveness of the model for $k_{rs}$ proposed in the previous section, for use over a wide range of aperture-field statistics and fluid properties, we simulated flow through fractures containing phase structures generated by systematically varying $C/\sigma$ [7]. The Gaussian, spatially correlated random aperture fields (1024x2048) used for these simulations obeyed a power spectrum of the form:

$$G\left(k_x, k_y\right) \quad \left(1 + l^2 k_x^2 + l^2 k_y^2\right)^{-n} \qquad (7)$$

where $k_x$ and $k_y$ are the wave numbers corresponding to the $x$ and $y$-dimensions, $n$ is an exponent in the range $1.0 \le n \le 1.5$, and $l$ is a cutoff length-scale [*18*]. This functional form of $G$ yields a smooth transition from the power law behavior ($|k|>1/l$) to the cutoff value ($|k|<1/l$) that results in random fields with well-behaved semivariograms (i.e. no oscillations as occur with an abrupt cutoff). The power law behavior for ($|k|>1/l$) corresponds to self-affine structure with Hurst exponent, $H=n-1$ [19]. For fields with zero mean, variance of 1 and $n$=1.3, $l$ was adjusted to yield a correlation length ($\lambda$) defined as the separation distance at which the semivariogram reached a value of $\sigma_a^2(1-1/e)$, of 5 grid-blocks. We generated six random fields and scaled each to yield fractures with $\sigma$= 0.0625, 0.125, and 0.25 resulting in a total of 18 aperture field realizations (**Fig. 1(a)**). Higher values of $\sigma$ yielded contact areas where the aperture is zero, which introduced additional complications during phase invasion and will not be addressed here.

In each of the 18 aperture fields, MIP was used to simulate wetting and nonwetting phase invasions for fourteen values of $C$ that began at 0, followed by 0.0021 with successive doubling up to 8.58, for a total of 504 simulations [7]. The invading phase was supplied across the entire edge of one short side of the random field while the defending phase was allowed to leave the field through the other three sides. Defending phase trapping was implemented and the simulation ended when all sites were either filled with invading phase or entrapped defending

phase. The results of the phase invasion simulations provided direct measurements of $S_f$, $A$, and $B$, but estimating $k_{rs}$ and $k_{rs\|}$ required flow simulations in the fractures.

We simulated flow within the satiated phase structures using the local cubic law, a depth-averaged approximation to the three-dimensional Stokes equations, given by:

$$\nabla \cdot \left[ \left( a^3 g / 12\nu \right) \nabla h \right] = 0 \qquad (8)$$

where $h$ is the local pressure head, $g$ is the gravitational constant, and $\nu$ is the kinematic viscosity of the flowing phase. No-flux boundary conditions were specified at the interfaces between the flowing and entrapped phases. We specified uniform constant pressure boundaries along the two short edges of the fractures and no flow boundaries along the long edges. The ratio of the simulated flow-rate in the satiated fracture to that in the saturated fracture provided an estimate of $k_{rs}$ for a fracture occupied by a specific phase distribution. Similar computations in a hypothetical parallel-plate fracture with impermeable obstructions corresponding to the entrapped phase geometry led to estimates of $k_{rs\|}$.

## IV. RESULTS

The results of the flow simulations demonstrate the influence of the entrapped phase on flow through satiated fractures. **Figure 1(b)-(h)** shows streamlines through fractures at several values of $C/\nu$ after both wetting and nonwetting invasions. For $C/\nu$=0 (**Fig. 1(b)**), the flowing phase occupies a small fraction of the total area, and the complex entrapped-phase structures result in large regions of flowing phase capturing very little of the total flow through the fracture. This is particularly evident in the center of the fracture where several large entrapped regions nearly block flow. As $C/\nu$ increases (**Fig. 1(c) and 1(d)**), the regions of entrapped defending phase become more compact leading to a larger number of open flow paths through the center of the fracture, less tortuous streamlines, and increased $k_{rs}$. Fundamental differences in the entrapped phase result during wetting and nonwetting invasions due to the order in which apertures are filled along the invading interface. **Figure 1(d) and (e)** demonstrates that wetting and nonwetting invasions at the same values of $C$ and $\nu$ lead to different entrapped regions within the same aperture field. Furthermore, $S_f$ is larger for the wetting invasion than the nonwetting invasion, which leads to slightly more tortuous streamlines for the nonwetting invasion.

The distributions of the apertures occupied by the invading fluid at satiation vary significantly for wetting versus nonwetting invasions (**Fig. 2**). For small values of $C/\nu$ there is little overlap between the distributions corresponding to the wetting and nonwetting invasions and they are almost symmetric about the mean aperture of the saturated fracture ($\bar{a}$=0.02 cm). However, as $C/\nu$ increases, the amount of overlap increases as a result of enhanced interface smoothing during invasion. Also, at larger values of $C/\nu$, the distributions are no longer symmetric about $\bar{a}$. This asymmetry is due to the asymmetric distribution of $1/a$ that corresponds to a Gaussian distribution for $a$. Because aperture-induced capillary pressure, which influences phase invasion, is proportional to $1/a$, asymmetry in the $1/a$ distribution leads to different behavior along the invading interface for wetting and nonwetting invasions. With a symmetric distribution for $1/a$, the aperture distributions for wetting and nonwetting invasions should be symmetric about $\bar{a}$ for all values of $C$ and $\nu$.

To evaluate the ability of the model presented in (3) to predict $k_{rs}$, we calculated the relevant parameters obtained from the 504 flow simulations. To clarify presentation of the data, for each combination of $C$ and $\nu$ we show only the average parameter values from the 6 aperture-field

realizations in the following plots. For each parameter, the standard deviation of the 6 measurements was no larger than 11% of the mean value and was typically less than 5%. This demonstrates that the influence of $C/\sigma$ on these parameters is more significant than variability across realizations. **Figure 3** shows $S_f$ plotted against $C/\sigma$, and shows, as detailed by Glass et al. [7], that $S_f$ exhibits a unique relationship with $C/\sigma$ for small values of $\sigma$. At larger values of $\sigma$ and $C/\sigma$ above ~0.5, measured values of $S_f$ fan apart and then converge again at large values of $C/\sigma$. Glass et al. [2003] explained this envelope based on the asymmetry in competition between smoothing and roughening, which is related to the asymmetric distribution of $1/a$. Based on the relationship between $C/\sigma$ and $S_f$ in **Fig. 3** a relationship that effectively quantifies $k_{rs}$ as a function of $S_f$ may be further generalized to directly relate $k_{rs}$ to $C/\sigma$.

The distribution of apertures occupied by the invading fluid during wetting and nonwetting invasions (**Fig. 2**) strongly influences measured values of $A$. **Figure 4** shows $A$ plotted against $S_f$ with the results of fitting (6) to each data set. The asymmetry in the distributions of aperture occupied by the invading fluid for the wetting and nonwetting invasions (**Fig. 2**) results in different values for the fitted parameter $b$: for nonwetting invasions $b$=4.59 and for wetting invasions $b$=3.98. The fitted curves for the wetting invasions deviate slightly from the data for intermediate values of $S_f$, but fit the data quite well for small values of $S_f$ where $A$ has the largest influence on estimates of $k_{rs}$.

**Figure 5** shows $k_{rs||}$ plotted against $S_f$ for all values of $C/\sigma$ and compares these results to (5), the proposed model of $k_{rs||}(S_f)$, with values of $S_{fl} = 0.72$, $S_f^* = 0.333$ and t = 1.3. The model fits the simulated values of $k_{rs||}$ quite well across the full range of $C/\sigma$ and only slightly overestimates the simulated values in the range of $0.55<C/\sigma<0.85$. The value of 0.72 for the parameter $S_{fl}$, which is related to the initial slope, was obtained based on a linear fit to simulated $k_{rs||}$ near $S_f = 1$. With t=1.3, $S_f^* = 0.333$ adequately represents the behavior of the simulated $k_{rs||}$ values for the smallest values of $S_f$. In the context of satiated phase structures, the percolation threshold parameter $S_f^*$ represents a lower bound for $S_f$ at satiation. All satiated phase structures must correspond to $S_f > S_f^*$; the lowest value observed in MIP simulations over numerous realizations of random aperture fields was 0.34 at the limit of $C/\sigma = 0$ (the mean value for $C/\sigma = 0$ over 36 realizations is 0.37). It is important to distinguish the above interpretation of $S_f^*$ from the actual value of $S_f$ at first breakthrough during IP, which is as low as 0.23 for $C/\sigma$=0, and around 0.8 at large values of $C/\sigma$. It is interesting to note that the value of 0.333 for $S_f$* corresponds to the percolation threshold for continuum percolation with circular or square holes [10,14,20], although the actual geometry of the entrapped phase (see Figure 1) is much more complicated, involving a wide range of sizes, shapes, orientations and aspect ratios. Garboczi et al. [14] investigated the variation of percolation threshold in mixed systems with circles of two different diameters, needles with two different lengths and circle-needle mixtures. Their results showed minor variations in the scaled percolation threshold invariant about their proposed universal value. We are unaware of any systematic results for continuum percolation with a broad distribution of size, shape and aspect ratios for the holes, for comparison with our estimate of $S_f$*. This appears to be an interesting problem for further investigation.

Using (5) and (6) to model $k_{rs||}$ and $A$ over the range of $S_f$ and $\sigma$ allows us to use (3) to estimate $k_{rs}$ over the full range of parameters. **Figure 6** compares the simulated values of $k_{rs}$ to estimates using (3). The deviations between the simulated results and the modeled estimates of $k_{rs}$ increase with $\sigma$ and are largest at intermediate values of $S_f$. The largest discrepancy between the measurements from the flow simulations and the model is a 25% difference between the modeled and simulated estimates of $k_{rs}$ for flow of a nonwetting fluid in the $\sigma$=0.25 fracture at $S_f$=0.56. For

smaller values of $\beta$, the discrepancies are a maximum of about 16% and are always somewhat larger for flow through phase structures resulting from nonwetting invasions.

## V. CONCLUSIONS

We have developed a model for predicting the satiated relative permeability across a broad range of entrapped phase structures in variable aperture fractures. These entrapped phase structures represent both wetting and nonwetting displacements over a full spectrum of possible Curvature numbers ($C$) and a comprehensive set of fracture aperture statistics ($\beta$). The resulting entrapped phase ranged from highly tortuous structures resulting from capillary fingering to compact smooth structures at large values of $C/\beta$. The satiated relative permeability ($k_{rs}$) was shown to depend on the product of $k_{rs\|}$, which quantifies the influence of the phase geometry alone, with additional factors that represent the modification of the aperture statistics due to selective occupancy by the flowing phase.

Our model for the satiated relative permeability ($k_{rs}$) uses well-established ideas from continuum percolation theory to relate $k_{rs\|}$ with $S_f$. This generalized model for $k_{rs\|}$ exhibits critical behavior for low $S_f$ (close to the percolation threshold) and linear behavior near $S_f$=1. The exponent in the power-law behavior at low $S_f$ is consistent with the universal conductivity exponent for two-dimensional percolation systems. The influence of aperture distribution and the effect of wetting versus nonwetting invasions on the mean aperture in the flowing phase are quantified through the term $A$. We have proposed a robust empirical relationship for $A$ in terms of $S_f$ and $\beta$. As expected, $A$ is greater than 1 for the non-wetting case and less than 1 for the wetting case and deviations from one are amplified by $\beta$. Thus, for a given value of $S_f$, $k_{rs}$ will be larger for flow of a nonwetting fluid than for a wetting fluid, with the difference enhanced at small values of $S_f$ and large values of $\beta$.

Comparison of the semi-empirical model for $k_{rs}$ to measurements of $k_{rs}$ resulting from flow simulations through 6 fracture realizations over a range of $C$ and $\beta$ demonstrate that the model predicts $k_{rs}$ quite well over the full range of parameters. It is somewhat surprising that the influence of the complex phase structures on permeability can be quantified as a function of a simple measure of the phase structure, such as $S_f$. However, it is likely that efforts to model other processes, such as solute transport in the flowing phase [21] or entrapped phase dissolution [22], will require higher order measures of the entrapped phase geometry. We note that the model relates $k_{rs}$ to $\beta$ and $S_f$, which in turn is fundamentally controlled by $C/\beta$ in the case of capillary-dominated displacements. Thus, for capillary-dominated displacements in a given fracture it is possible to estimate $k_{rs}$ directly if the fracture aperture statistics and contact angle at the interface (i.e. $C$, $\beta$ and $\theta$) are known.

## ACKNOWLEDGMENTS

Funding for this work was provided by the US Department of Energy's Office of Basic Energy Sciences, Geosciences Program under contract numbers DE-FG03-96ER14590 (University of Colorado), DE-AC04-94AL85000 (Sandia National Laboratories), and W-7405-Eng-48 (University of California, Lawrence Livermore National Laboratory).

## REFERENCES


[1] K. Pruess and Y. W. Tsang, Water Resour. Res. **26**, 1915 (1990).
[2] M. Fourar, S. Bories, R. Lenormand, P. Persoff, Water Resour. Res. **29**, 3699 (1993).
[3] J.R. Murphy and N.R. Thomson, Water Resour. Res. **29**, 3453 (1993).
[4] P. Persoff and K. Pruess, Water Resour. Res. **31**, 1175 (1995).
[5] R.J. Glass, L. Yarrington, and M.J. Nicholl, Water Resour. Res. **34**, 3215 (1998); **36**, 1991 (2000).
[6] M.J. Nicholl, H. Rajaram, and R.J. Glass, Geophys. Res. Lett. **27**, 393 (2000).
[7] R.J. Glass, H. Rajaram, and R.L. Detwiler, Phys. Rev. E **68**, 061110 (2003).
[8] L.D. Landau and E.M. Lifshitz, *Electrodynamics of continuous media* (Pergamon, New York, 1960).
[9] R.W. Zimmerman and G.S. Bodvarsson, Trans. Porous Media **23**, 1 (1996).
[10] G.E. Pike and C. H. Seager, Phys. Rev. B **10**, 1421 1974
[11] B.I. Halperin, S. Feng and P. N. Sen, Phys. Rev. Lett. **54**, 2391, 1985
[12] S. Feng, B. I. Halperin, P. N. Sen, Phys. Rev. B **35**, 197, 1987
[13] W. Xia and M. F. Thorpe, Phys. Rev. A **38**, 2650, 1988
[14] E.J. Garboczi, M.F. Thorpe, M.S. Devries, and A.R. Day, Phys. Rev. A **43**, 6473 (1991).
[15] D. Stauffer and A. Aharony, *Introduction to Percolation Theory*, ed. 2. (Taylor and Francis, London, 1992).
[16] M. Sahimi, *Flow and Transport in Porous Media and Fractured Rock*, (VCH, Weinheim, 1995).
[17] J. Tobochnik, M. A. Dubson, M. L. Wilson, M. F. Thorpe, Phys. Rev. A **40**, 5370, 1989
[18] S.R. Brown, J. Geophys. Res. **100**(B4), 5941 (1995).
[19] P.M. Adler and J.-F. Thovert, *Fractures and Fracture Networks*, (Kluwer, Boston, 2000).
[20] E. T. Gawlinski and H. E. Stanley, J. Phys. A **14**, L 291, 1981
[21] R.L. Detwiler, H. Rajaram, and R.J. Glass, Geophys. Res. Lett. **29**, 1 (2002).
[22] R.L. Detwiler, H. Rajaram, and R.J. Glass, Water Resour. Res. **37**, 3115 (2001).

**Figure Captions**

**Figure 1:** Aperture field and example of satiated phase structure and flow paths: a) Aperture field for $\sigma$=0.25 where gray scale reflects apertures ranging from zero (black) to the maximum of 0.045 cm (white); b) wetting invasion, $C$=0, $\sigma$=0.0625 (IP), $S_f$~0.38; c) wetting invasion, $C$=0.0335, $\sigma$=0.0625, $C/\sigma$=0.536, $S_f$~0.51; d) wetting invasion, $C$=0.134, $\sigma$=0.0625, $C/\sigma$=2.144, $S_f$~0.74; and e) nonwetting invasion, $C$=0.134, $\sigma$=0.0625, $C/\sigma$=2.144, $S_f$~0.69. Invasion was from left to right; dark gray regions represent defending phase entrapped within the rough-walled fracture, white regions represent the location of the invading phase at breakthrough (i.e. percolation threshold), light gray regions represent additional locations occupied by the invading phase at satiation, and black shows the trajectory of 25 particles released along the inflow edge of the fracture. The initial particle spacing was flux weighted.

**Figure 2:** Distributions of apertures occupied by the invading phase at satiation for both wetting (open symbols) and nonwetting (filled symbols) invasions. The thick solid line represents the aperture distribution for the saturated fracture.

**Figure 3:** Average $S_f$ for six realizations plotted against $C/\sigma$ for both wetting (open symbols) and nonwetting (filled symbols) invasions.

**Figure 4:** $A$ plotted against $S_f$ for all values of $\sigma$ for both wetting (open symbols) and nonwetting (filled symbols) invasions.

**Figure 5:** $k_{rs\|}$ plotted against $S_f$ for all values of $\sigma$ for both wetting (open symbols) and nonwetting (filled symbols) invasions.

**Figure 6:** $k_{rs}$ measured from flow simulations plotted against $k_{rs}$ estimated using (3) for both wetting (open symbols) and nonwetting (filled symbols) invasions.

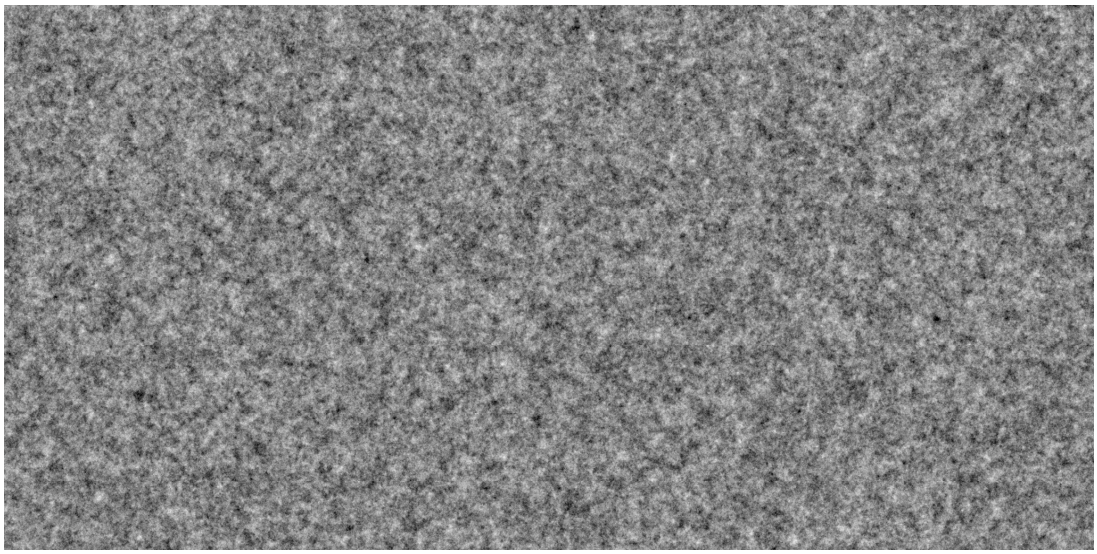

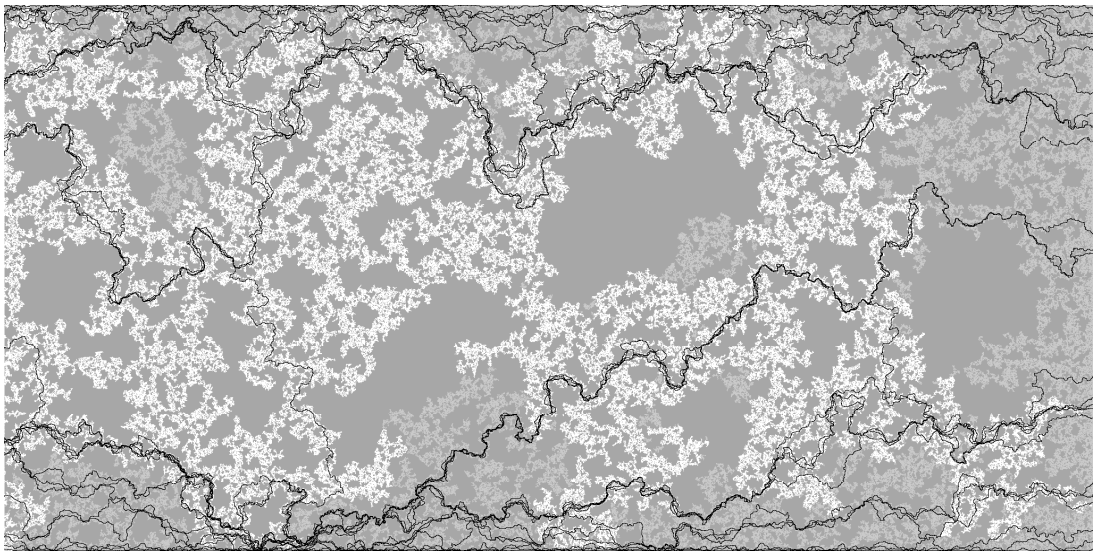

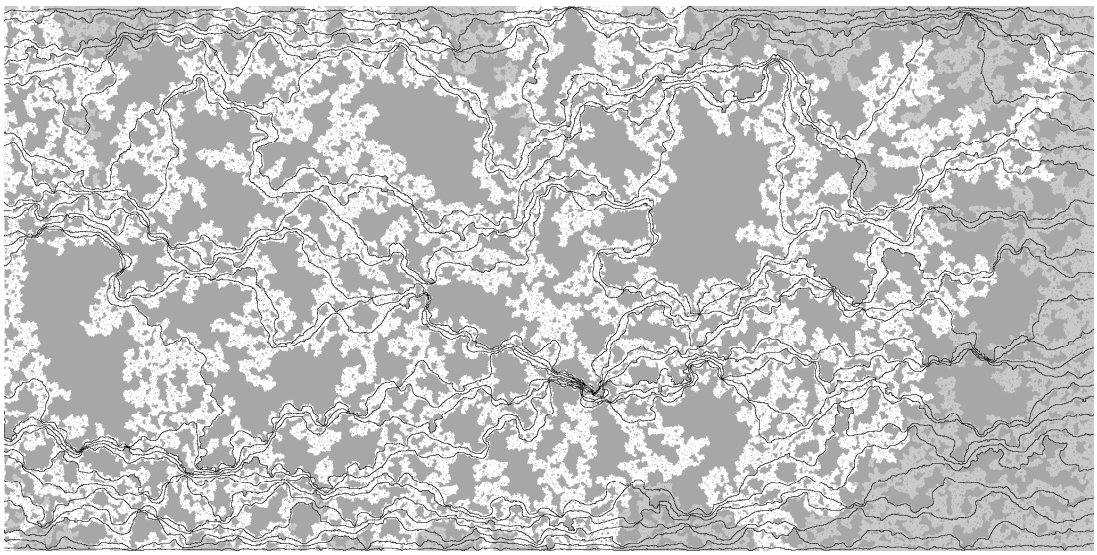

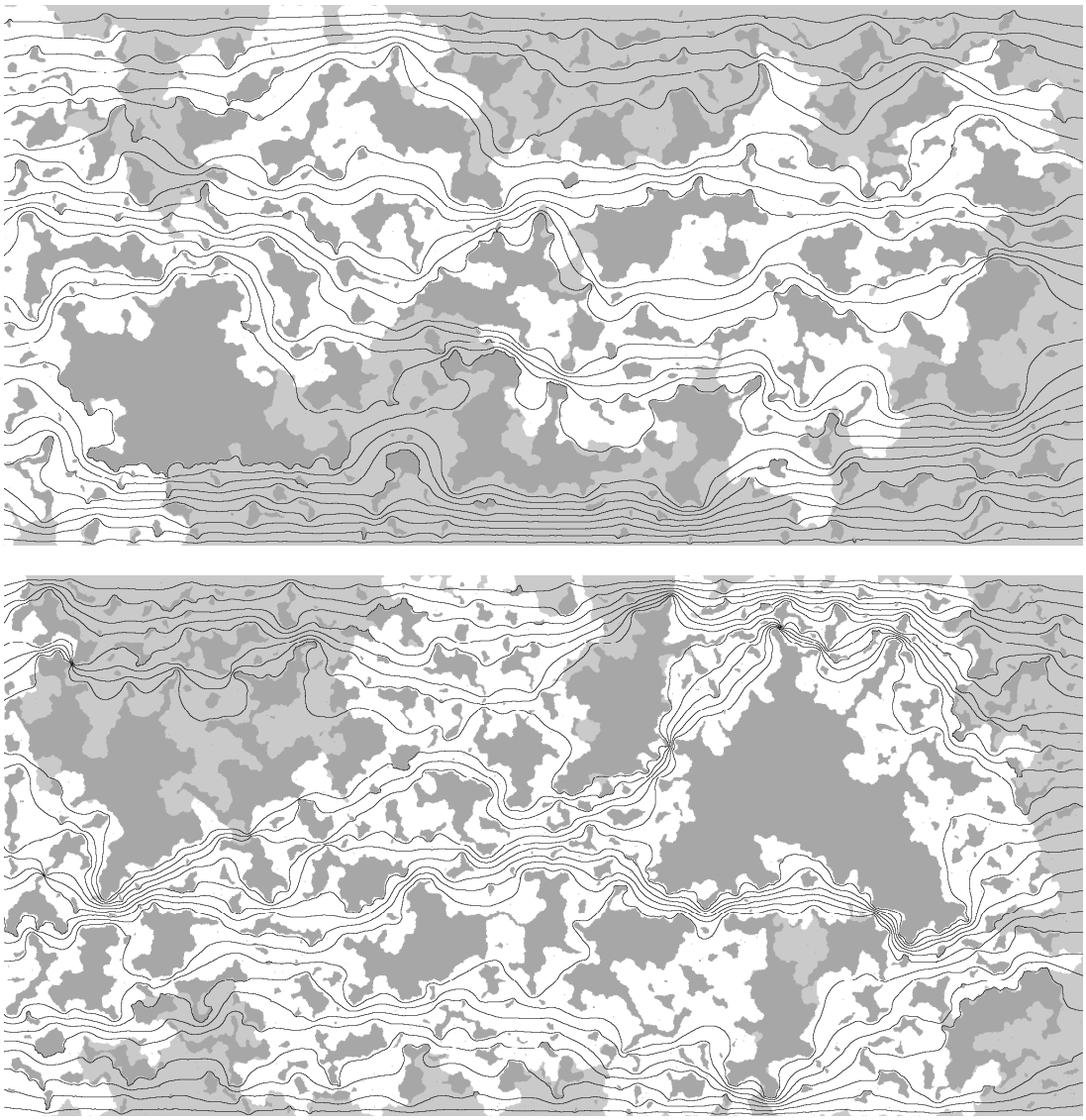

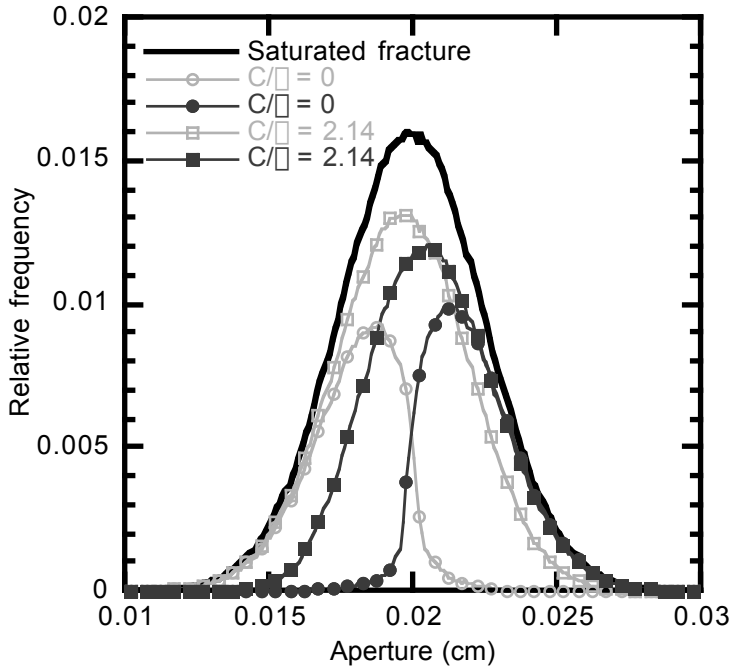


Figure 2:

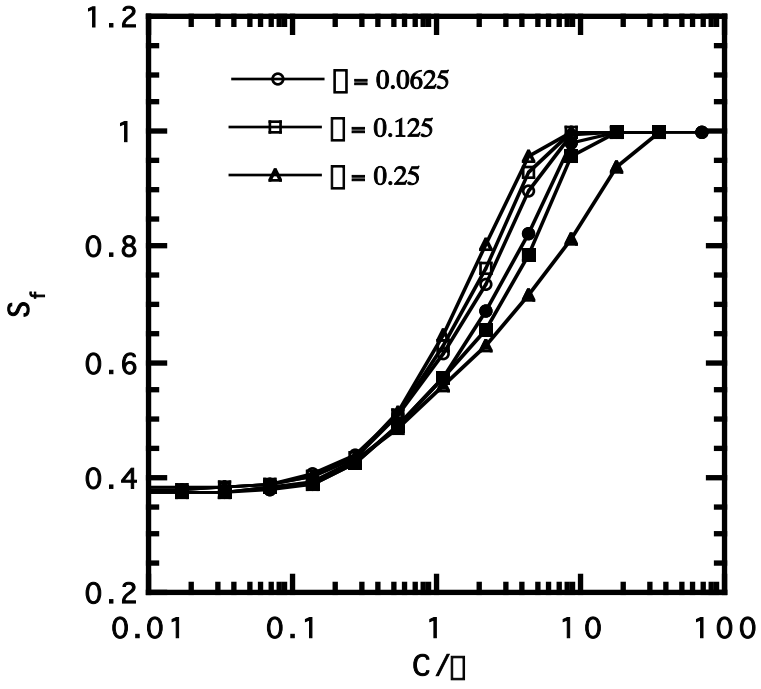


Figure 3:

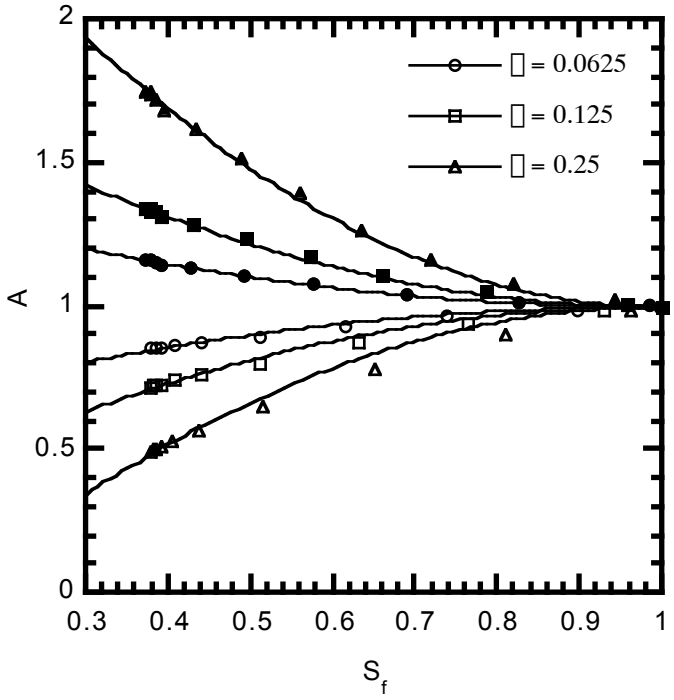


Figure 4:

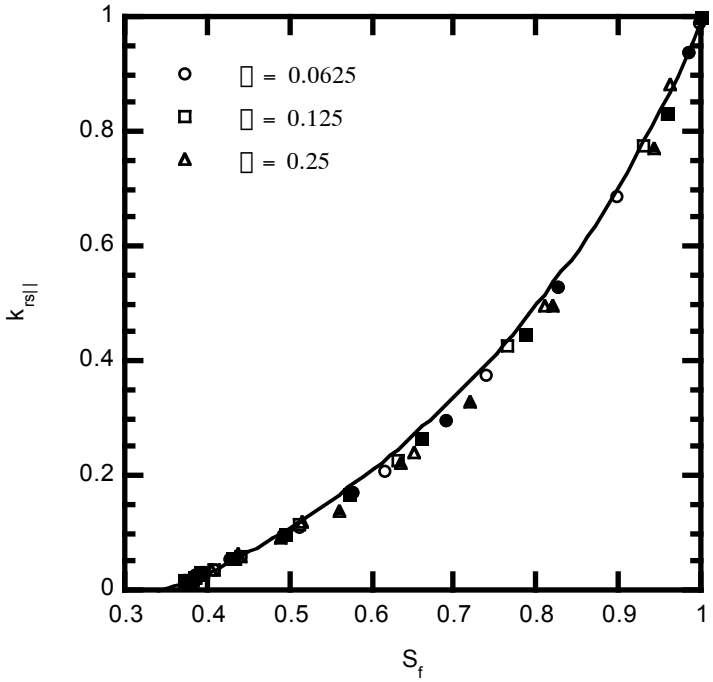


Figure 5:

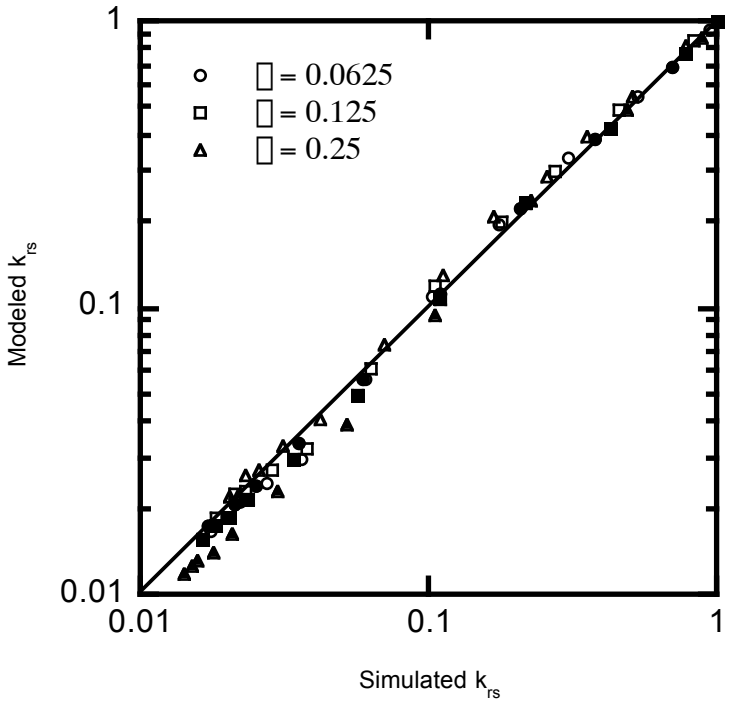


Figure 6: